Ab Initio Molecular Orbital Study of the Reactivity of Active Alkyl Groups. VI. Modified Reaction Model for the Elimination Process of Nitrosation Reaction

Hirohito IKEDA, Miho YUKAWA, and Tokihiro NIIYA*

Faculty of Pharmaceutical Sciences, Fukuoka University; Nanakuma, Jonan-ku, Fukuoka 814–0180, Japan.
Received December 24, 2004; accepted March 26, 2005

The mechanisms of nitrosation of acetone through sodium enolate $[CH_3COCH_2]^-Na^+$ (1) or naked enolate $[CH_3COCH_2]^-$ (2) with *tert*-butyl nitrite $(CH_3)_3CONO$ (3) were studied using *ab initio* molecular orbital (MO) methods. When the modified complex model was used in the elimination process, our results demonstrated the predominant formation of *E*-1-hydroxy-imino-2-oxo-propane $CH_3COCH{=}NOH$ (4*E*), in which a counter-cation of the base catalyst did not participate during the reaction. On the other hand, participation of the counter-cation during the reaction contributed to the formation of the *Z*-isomer of 4 (4*Z*).

Key words nitrosation; active alkyl group; reaction mechanism; *ab initio* molecular orbital (MO) method; stereochemistry; oxime

The nitrosation of an active alkyl compound ($RCOCH_2R'$) with an alkyl nitrite (R″ONO) can be expressed by the following equations[1—3]:

$$RCOCH_2R' + B^-M^+ \rightarrow [RCOCHR']^-M^+ + BH \quad (1)$$

$$[RCOCHR']^-M^+ + R''ONO \rightarrow [RCOCHNO(OR'')R']^-M^+ \quad (2)$$

$$[RCOCHNO(OR'')R']^-M^+ + B^- \rightarrow [RCOC(=NO)R']^-M^+ + [R''O]^- + BH \quad (3)$$

The abstraction of the active hydrogen of $RCOCH_2R'$ by a base catalyst B^-M^+, and the subsequent formation of the enolate $[RCOCHR']^-M^+$ are described in Eq. 1 (deprotonation process). Secondly, the creation of a C–N bond, in which $[RCOCHR']^-M^+$ reacts with R″ONO to form complex $[RCOCHNO(OR'')R']^-M^+$, is shown in Eq. 2 (C–N bond formation process). Finally, the reaction between $[RCOCHNO(OR'')R']^-M^+$ with base catalyst B^-, then deprotonation and elimination of the $[R''O]^-$ group from $[RCOCHNO(OR'')R']^-M^+$ to form the oxime anion $[RCOC(=NO)R']^-M^+$ is presented in Eq. 3 (elimination process). Among the three processes, the rate-determining step in the nitrosation is the C–N bond formation process. The structure of the transition state (TS) of the C–N bond formation process is reflected as the ratio (*E*/*Z*) of the *E*- and *Z*-isomers of the resulting oxime. In a previous paper, two TS models, "metal-chelated pericyclic TS" ($TS_{CHELATED}$) and "open-chain TS without metal" (TS_{OPEN}), were presented to explain the change in the *E*/*Z* ratio as the reaction changed from aprotic solvent to protic solvent conditions.[1—3]

In this report, the stereochemical reaction mechanisms using two types of TS models during the nitrosation of **1** or **2** with **3** (shown in Eq. 4) were studied using an *ab initio* molecular orbital (MO) method. Differences in the calculations between the previous and present studies are attributable to: **1**) *tert*-butyl nitrite being used instead of methyl nitrite, **2**) following the reaction *via* TS_{OPEN} during the C–N bond formation process, the subsequent elimination with the base proceeding without the participation of the counter-cation of the base, and **3**) during the intrinsic reaction coordinate (IRC) calculations for the elimination process, not fixing the bond and dihedral angles in the geometric parameter of the hydrogen atom, which is attacked by the base catalyst, at 90 degrees.

$$\underset{\textbf{1 or 2}}{[CH_3COCH_2]^-M^+} + \underset{\textbf{3}}{(CH_3)_3CONO} \xrightarrow{CH_3O^-} \underset{\textbf{4}}{[CH_3COCH{=}NO]^-M^+} + (CH_3)_3COH \quad (4)$$

Experimental

Computational Procedures MO calculations were carried out using the Gaussian98 program.[4,5] The optimized geometries in the TS were initially determined using HF/6-31G, followed by IRC calculations. For the energies of the complexes, calculations were performed using similar methods, MP3/6-31+G//HF/6-31G as previously described.[1—3] The vibrational modes of all transition states were confirmed by frequency analysis.

Results and Discussion

As described in the previous paper,[1—3] MO calculations for the nitrosation of **1** or **2** were carried out stepwise as shown in Chart 1.

For the C–N bond formation process, the $TS_{CHELATED}$ and TS_{OPEN} models were used. The geometrical and energy calculations of the complexes produced in reaction paths A and B were performed using the orientation of **3** shown in Fig. 1. Using the IRC method, the geometries of $C\text{-}I_{(Na)}$ and $C\text{-}II_{(Na)}$ were determined based on that of $TS1_{(Na)}$, which was initially determined.

In the elimination process, either hydrogen atom H^1 or H^2 on the C^2 atom of $C\text{-}II_{(Na)}$ is initially attacked by a base, CH_3O^-. The release of the $[(CH_3)_3CO^3]^-$ group from **3** and the deprotonation of either the H^1 or H^2 atom of $C\text{-}II_{(Na)}$ yields the corresponding oxime. Using IRC calculations, the geometries of $C\text{-}III_{Na}$ and $C\text{-}IV_{Na}$ were obtained, based on that of $TS2_{Na}$. Although IRC calculations were carried out to obtain the geometries of C-III and C-IV from TS2, the transient optimized complexes were not obtained due to the electric repulsion between the CH_3O^- and $[CH_3COCH_2NO(OC(CH_3)_3)]^-$ in C-III or the $[(CH_3)_3CO]^-$ and $[CH_3COCH{=}NO]^-$ in C-IV.

C–N Bond Formation of the Sodium Enolate of Ace-

* To whom correspondence should be addressed. e-mail: niiya@fukuoka-u.ac.jp

C-N Bond Formation Process

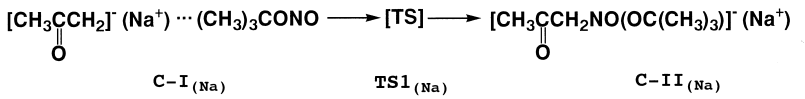

Elimination Process

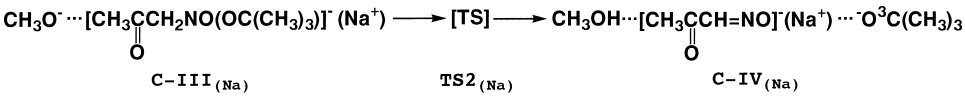

Chart 1

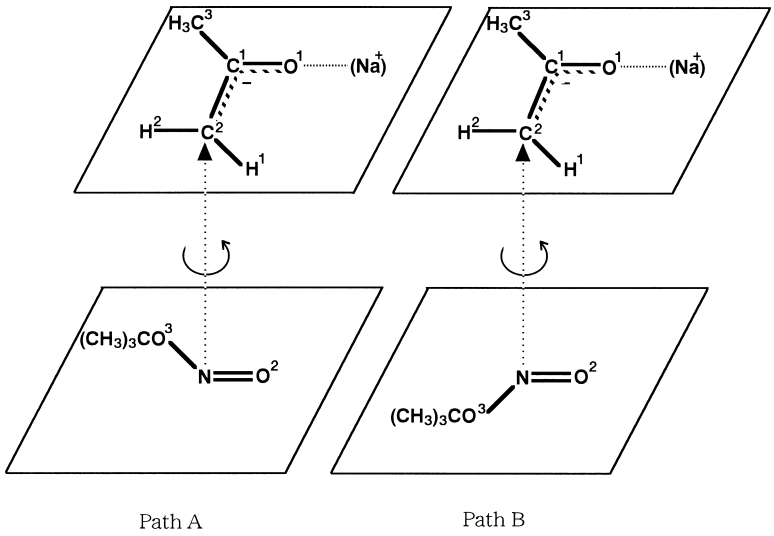

Fig. 1. Orientation of *tert*-Butyl Nitrite towards Enolate of Acetone for Energy Calculation of C–N Bond Formation

tone with *tert*-Butyl Nitrite *via* $TS_{CHELATED}$ The optimized geometries, bond lengths (Å), and calculated energies of C-I_{Na}, $TS1_{Na}$ and C-II_{Na} of both paths A and B are shown in Fig. 2. The Na^+ atom of C-I_{Na} coordinates to the O^1, O^2, and O^3 atoms, whereas that of $TS1_{Na}$ coordinates to the O^1 and O^2 atoms to form a 6-membered ring. The differences between the energies of C-I_{Na} and $TS1_{Na}$-A or $TS1_{Na}$-B, *i.e.*, the activation energies (E_a) during the C–N bond formation process, are 8.33 kcal mol^{-1} or 9.52 kcal mol^{-1}, respectively. As a note, the activation energy of path A is smaller than that of path B. During the transformation of C-I_{Na} to C-II_{Na}, the structure of **1** changes from the enol- to the keto-form, and the hybridization of the C^2 atom changes from sp^2- to sp^3-type. The Na^+ atom coordinates to the O^1, O^2, and O^3 atoms of C-II_{Na}-A, whereas that of C-II_{Na}-B coordinates to the O^1 and O^2 atoms. Comparatively, the geometry of C-II_{Na}-A is more stable than that of C-II_{Na}-B. The bond lengths of N–O^3 of C-II_{Na}-A and C-II_{Na}-B are 1.486 Å and 1.441 Å, respectively. Consequently, between the available paths, path A was more favorable in the C–N bond formation *via* $TS_{CHELATED}$. In this process, the oxime was yet to be produced.

The geometries of the complexes during the C–N bond formation process of nitrosation of **1** with *tert*-butyl nitrite are comparable to those of **1** with methyl nitrite.[1)] In the case of *tert*-butyl nitrite, the bulkiness of the $(CH_3)_3C$ group did not contribute to the regulation of the formation of oxime isomers.

C–N Bond Formation of the Enolate Anion of Acetone with *tert*-Butyl Nitrite *via* TS_{OPEN} The optimized geometries, bond lengths (Å), and energies of C-I, TS1, and C-II in paths A and B are shown in Fig. 3. Due to the electronic repulsion between the O^1 and O^2 atoms, the direction of the coordinates of these O atoms toward the C^2–N axis is reversed for TS1. Comparatively, the E_a of path A is 7.32 kcal mol^{-1} and that of path B is 4.98 kcal mol^{-1}, in which the reaction *via* path B occurs more readily than that *via* path A. As the reaction proceeds from C-I to C-II *via* TS1, the length of the C^1–O^1 bond shortens and, although that of N–O^3 gradually becomes longer, the N–O^3 bond does not cleave. The dihedral angle $\angle C^4O^3NO^2$ of C-II is about 90 degrees (path A) or −90 degrees (path B); in other words, the conformation of the $(CH_3)_3C^4O^3NO^2$ moiety changes from the *anti*-form to the *syn*-form.

The optimized conformations of the complexes in the C–N bond formation process of path B are similar to those of **1** with methyl nitrite.[2)] In contrast, the optimized conformations of C-II-A and -B are somewhat different than the corresponding conformations of C-II-A and -B that were calculated with methyl nitrite.[2)] Presumably, during the process, the contribution of the bulky $(CH_3)_3C$ group was merely to stabilize the conformation of C-II.

Elimination of Proton and *tert*-Butoxide in C-II_{Na}-A with a Base The deprotonation of either the H^1 or H^2 atom and the cleavage of the N–O^3 bond in C-II_{Na}-A are both necessary in the formation of the corresponding oxime. It is well known that an E2 reaction occurs readily *via* an antiperipla-

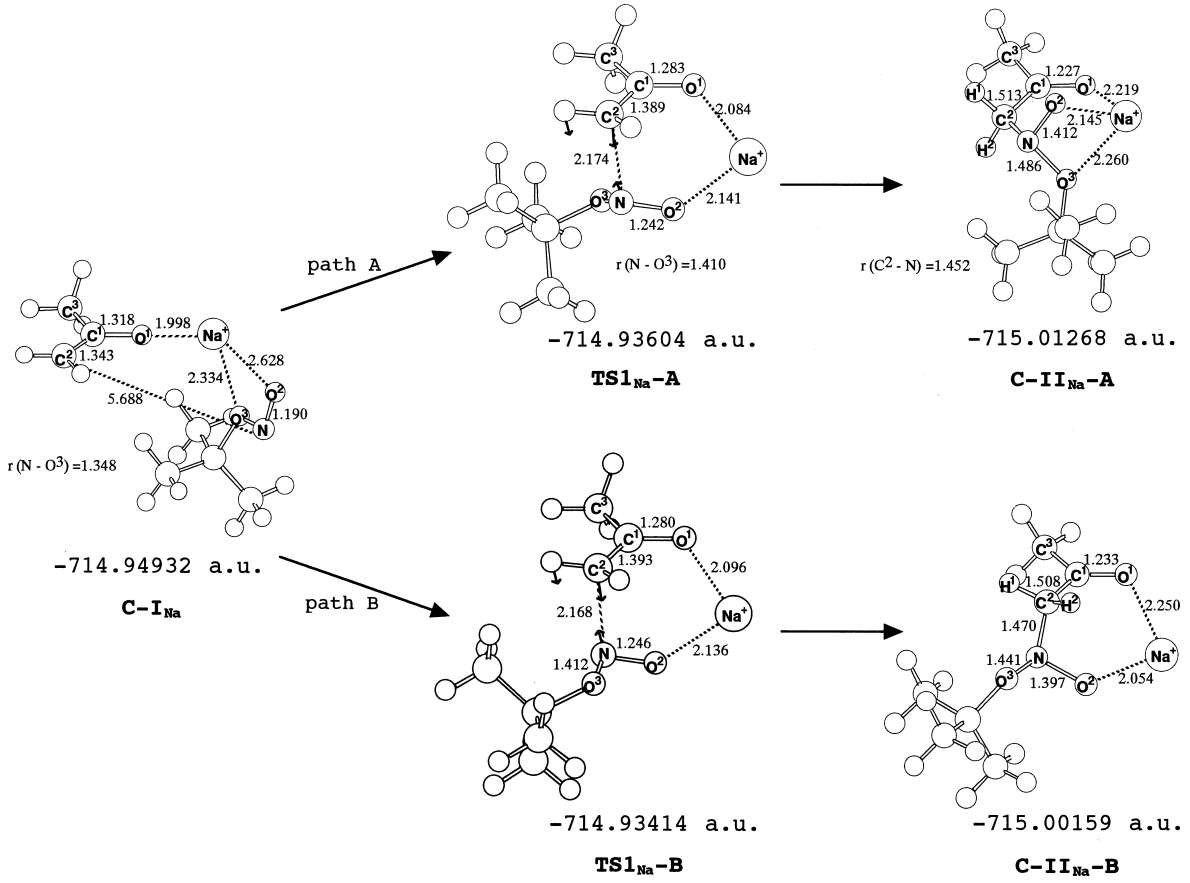

Fig. 2. C–N Bond Formation Process of Nitrosation of $[CH_3COCH_2]^-Na^+$ with $(CH_3)_3CONO$ *via* $TS1_{Na}$
Imaginary frequency modes are shown with bold arrows in the structures of the transition states.

nar geometry, which is defined as leaving groups that lie in the same plane.[6] In the case of C-II_{Na}-A, the two leaving groups, the H^1 atom and the $(CH_3)_3CO^3$ fragment, are arranged nearly antiperiplanar to each other. Consequently, it is reasonable to propose an elimination model in which the oxygen atom of the CH_3O^- base approaches the H^1 atom along the axis of the C^2–H^1 bond. The optimized geometries, bond lengths (Å), and energies of C-III_{Na}-AH^1, $TS2_{Na}$-AH^1, and C-IV_{Na}-AH^1 are shown in Fig. 4. The frequency mode of the $TS2_{Na}$-AH^1 complex shows that the transition state of the deprotonation differs from that of the cleavage of the N–O^3 bond during the elimination process of the nitrosation of sodium enolate $[CH_3COCH_2]^-Na^+$ (**1**) with methyl nitrite CH_3ONO. In contrast, the *tert*-butyl group of **3** prevents the cleavage of the N–O^3 bond during the elimination process. Upon comparison of the energies of C-III_{Na}-AH^1 and $TS2_{Na}$-AH^1, the value of E_a for the deprotonation is 3.31 kcal mol^{-1}. Although the C^2–H^1 bond was elongated with the approach of the CH_3O^- base to the H^1 atom, the bond length of N–O^3 did not increase in the case of C-IV_{Na}-AH^1, *i.e.*, the desired oxime was not formed. During this process, in contrast to the elimination process during the nitrosation of **1** with methyl nitrite, the bulkiness of the $(CH_3)_3C$ group contributed to prevent the cleavage of the N–O^3 bond of C-II_{Na}-A.

Elimination of Proton and *tert*-Butoxide in C-II_{Na}-B with a Base In the case of C-II_{Na}-B, the two leaving groups, $H^{1\,(or\,2)}$ and $(CH_3)_3CO^3$, were not arranged so as to be nearly antiperiplanar to one another. At first, the reaction of H^1 of C-II_{Na}-B with CH_3O^- was studied. The frequency mode of $TS2_{Na}$-BH^1 indicates the transition state during the deprotonation. The activation energy E_a is 7.20 kcal mol^{-1}. During the deprotonation of H^1 of the C^2 atom, elimination of the $(CH_3)_3CO^3$ group did not occur, and hence the oxime product was not afforded.

Next, deprotonation of the H^2 atom of C-II_{Na}-B with CH_3O^- was investigated. The optimized geometries, bond lengths (Å), and energies of C-III_{Na}-BH^2, $TS2_{Na}$-BH^2, and C-IV_{Na}-BH^2 are shown in Fig. 5. The frequency mode of $TS2_{Na}$-BH^2 shows the transition state during the deprotonation. The energy E_a was 1.28 kcal mol^{-1}. In the case of C-IV_{Na}-BH^2, the deprotonation caused the cleavage of the N–O^3 bond to afford **4***Z*, which is different from the case of the deprotonation of the H^1 atom in C-II_{Na}-B.

In a previous study of the mechanism of nitrosation *via* the "Open-Chain" transition state, the model complex (C-II—Na^+), in which counter-cation Na^+ of the base was coordinated to an oxygen atom, was used as the initial structure for the elimination process. In the present study, initial complexes C-II-A or -B without a counter-cation Na^+ were used as the modified model for the elimination process, as described below.

Elimination of Proton and *tert*-Butoxide in C-II-A with a Base In the case of C-II-A, the $H^{1\,(or\,2)}$ atom and the $(CH_3)_3CO^3$ group were not located in an antiperiplanar arrangement. At first, the transition state for the elimination was decided. The optimized complex TS2-AH^1 was chosen

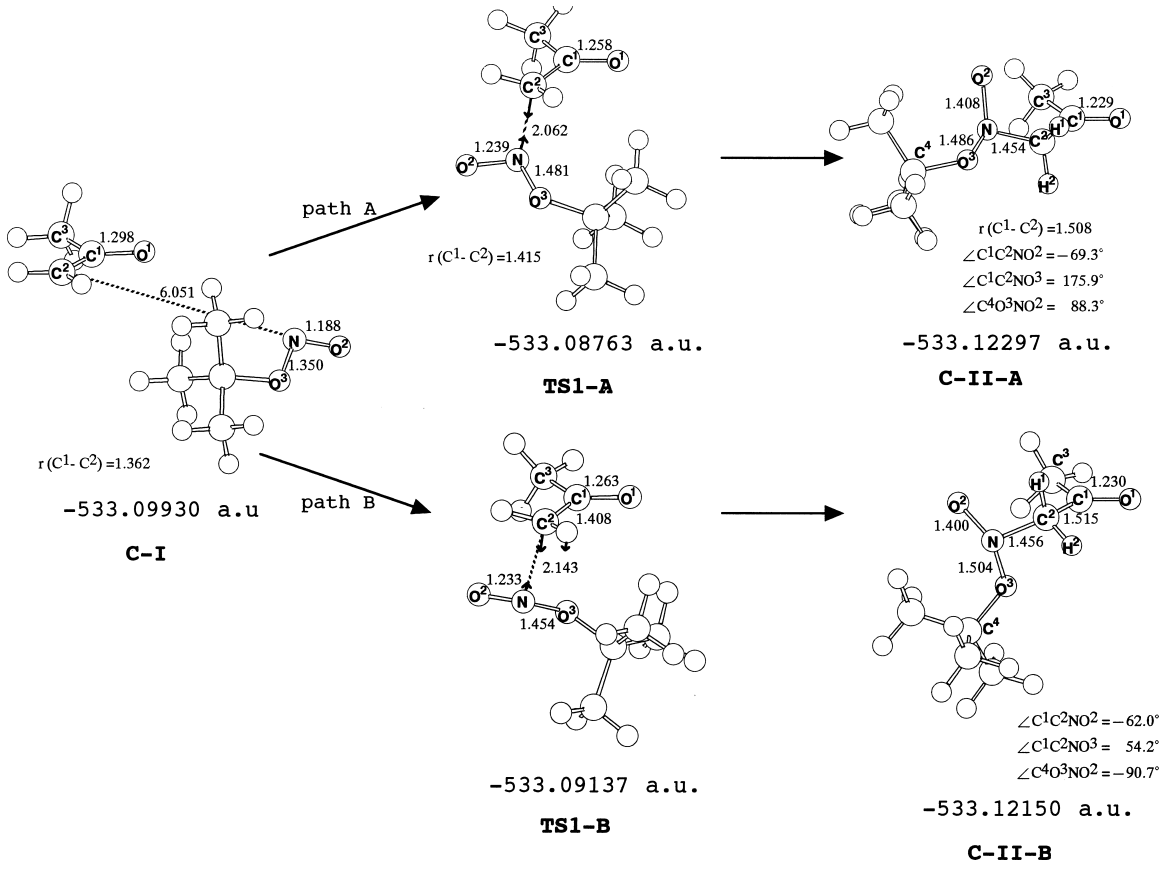

Fig. 3. C–N Bond Formation Process of Nitrosation of $[CH_3COCH_2]^-$ with $(CH_3)_3CONO$ *via* TS1

Imaginary frequency modes are shown with bold arrows in the structures of the transition states.

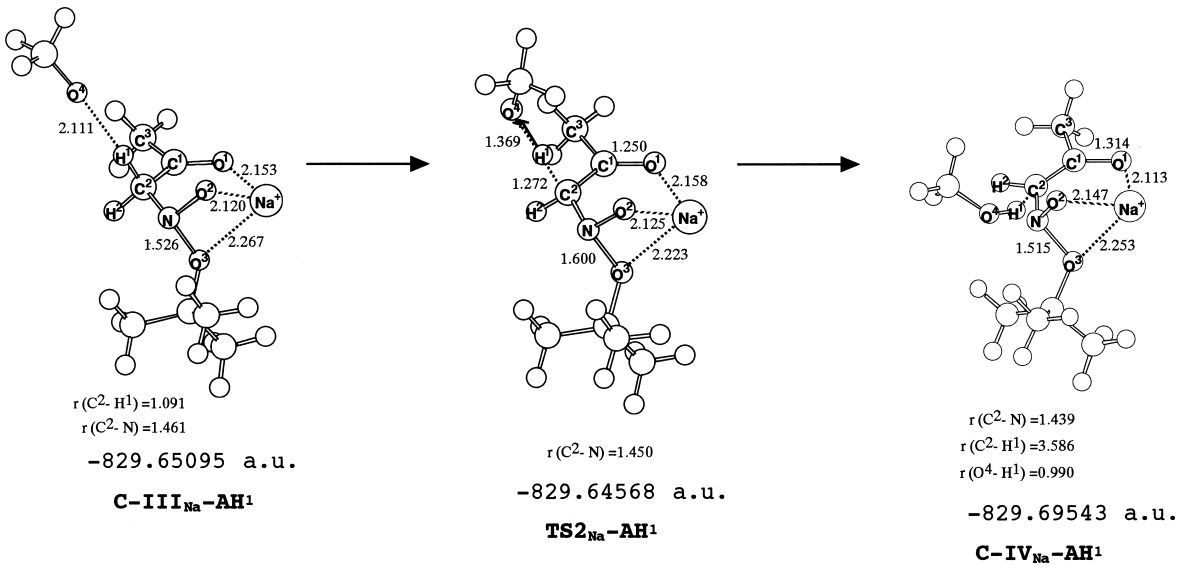

Fig. 4. Elimination Process of H^1 in C-II$_{Na}$-A with CH_3O^-

Imaginary frequency mode is shown with bold arrows in the structure of the transition state.

as the transition state of the deprotonation. Calculations for the geometries of C-III-AH^1 and C-IV-AH^1 were carried out using the IRC method. The results using the TS2-AH^1 were not similar to those obtained using TS2$_{Na}$-AH^1. Two types of anions, the CH_3O^- base and C-II ($[CH_3COCH_2NO(OC(CH_3)_3)]^-$) or the elimination group $[(CH_3)_3CO]^-$ and the product fragment $[CH_3COCHNO]^-$ produced in the reaction, were significantly far away from each other due to electronic repulsion effects. For these reasons, the minimized geometries of C-III-AH^1 and C-IV-AH^1 were not obtained using IRC methods. The optimized geometries, bond lengths (Å), and energies of TS2-AH^1 and C-IV-AH^1, in which the length of the O^4–H^1 bond is 0.960 Å, are shown in Fig. 6. The desired complex C-IV-AH^1, which

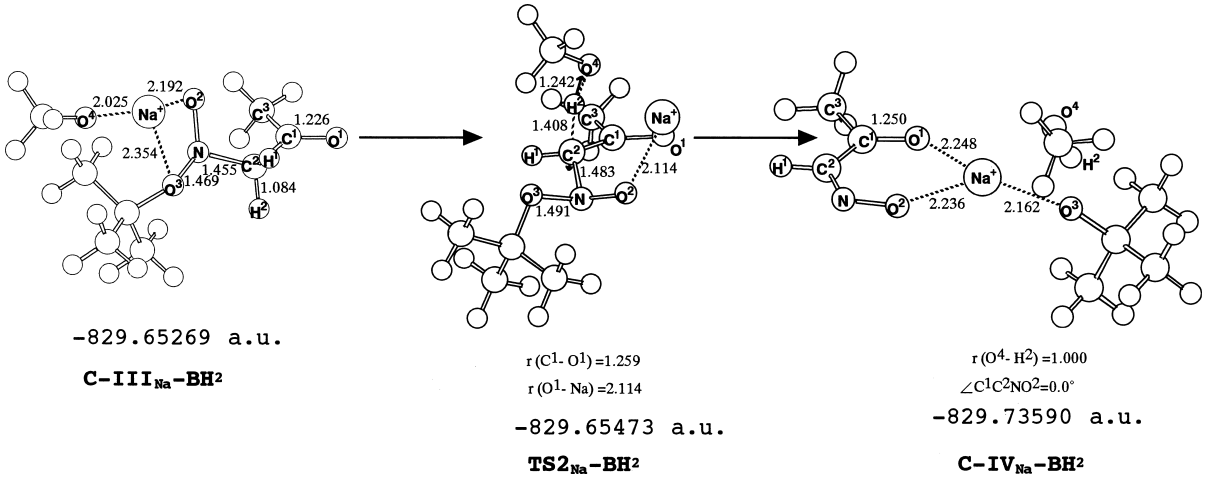

Fig. 5. Elimination Process of H^2 in C-II$_{Na}$-B with CH_3O^-

Imaginary frequency mode is shown with bold arrows in the structure of the transition state.

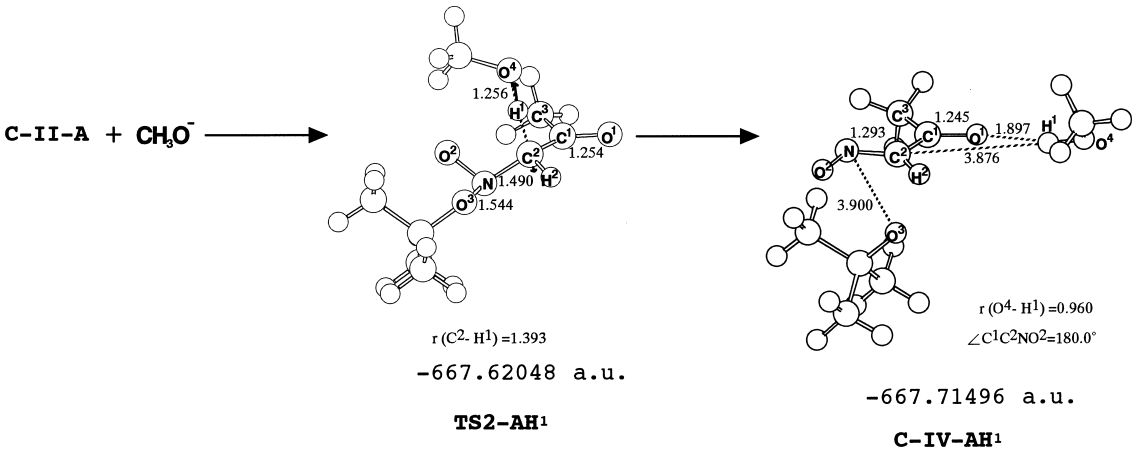

Fig. 6. Elimination Process of H^1 in C-II-A with CH_3O^-

Imaginary frequency mode is shown with bold arrows in the structure of the transition state.

was comprised of oxime **4***E*, was afforded using IRC calculations. In the same manner, the reaction between the CH_3O^- base and the H^2 atom of C-II-A was studied. The optimized geometries, bond lengths (Å), and energies of TS2-AH^2 and C-IV-AH^2, in which the length of the O^4–H^1 bond is 0.950 Å, are shown in Fig. 7. The desired complex C-IV-AH^2, which was comprised of oxime **4***E*, was afforded using IRC calculations. The reaction mechanism *via* TS2-AH^2 in the formation of **4***E* was very similar to that *via* TS2-AH^1.

Using an aprotic solvent, *Z*-oxime is predominantly obtained in the nitrosations, in which the counter-cation of the base catalyst contributes greatly to the reaction. On the other hand, *E*-oxime tends to form for nitrosations using a protic solvent, in which the counter-cation scarcely participates in the reaction. The conformation of the oxime, therefore, is decided by the extent that the counter-cation contributes to the C–N bond formation and the elimination processes of nitrosation.

Elimination of Proton and *tert*-Butoxide in C-II-B with a Base In the structure of C-II-B, the two leaving groups, H^1 and $(CH_3)_3CO^3$, are nearly antiperiplanar to each other. In order to determine the geometry of TS2-BH^1, the deprotonation of the H^1 atom with the $(CH_3O^4)^-$ base was investigated. The geometry of the transition state could not be determined using the usual method. The operations of the optimization procedure were performed stepwise: shortening of the length of the O^4–H^1 bond, followed by calculating the transition state. In the process, both elimination of $[(CH_3)_3CO^3]^-$ and deprotonation of the H^1 atom from C-II-B occurred readily to afford complex C-IV′-BH^1. The optimized conformation of the apparent transition state (TS2′-BH^1; the structure with two imaginary freqencies), in which the length of the O^4–H^1 bond is 1.720 Å, is shown in Fig. 8. The generation of **4***E* was confirmed for C-IV′-BH^1.

Conclusion

For complex C-II$_{(Na)}$, the attack of a base on the H atom of the C^2 atom is necessary for the formation of the corresponding oxime. For the elimination process, deprotonation in the presence of a base resulted predominantly in the cleavage of the N–O^3 bond in C-II$_{(Na)}$. The results of our studies clarified the influence of the counter-cation of the base catalyst on the conformation of the *E*-oxime.

Comparisons among the E_a values for each path of the C–N bond formation process revealed that path B *via* TS_{OPEN} kinetically proceeds to easily give *E*-oxime.

For the nitrosation reactions using modified models, complexes C-II-A or -B that are not coordinated to a Na^+

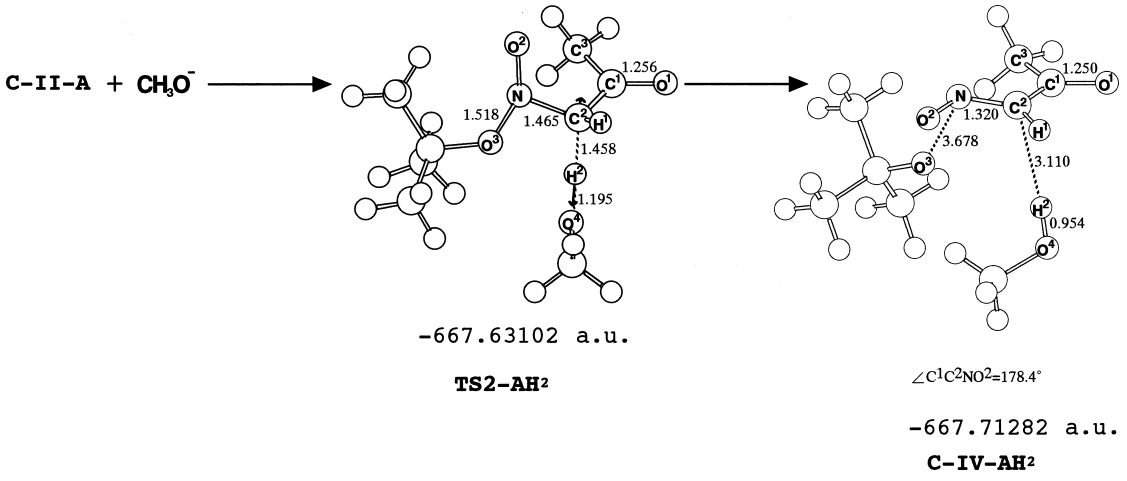

Fig. 7. Elimination Process of H^2 in C-II-A with CH_3O^-

Imaginary frequency mode is shown with bold arrows in the structure of the transition state.

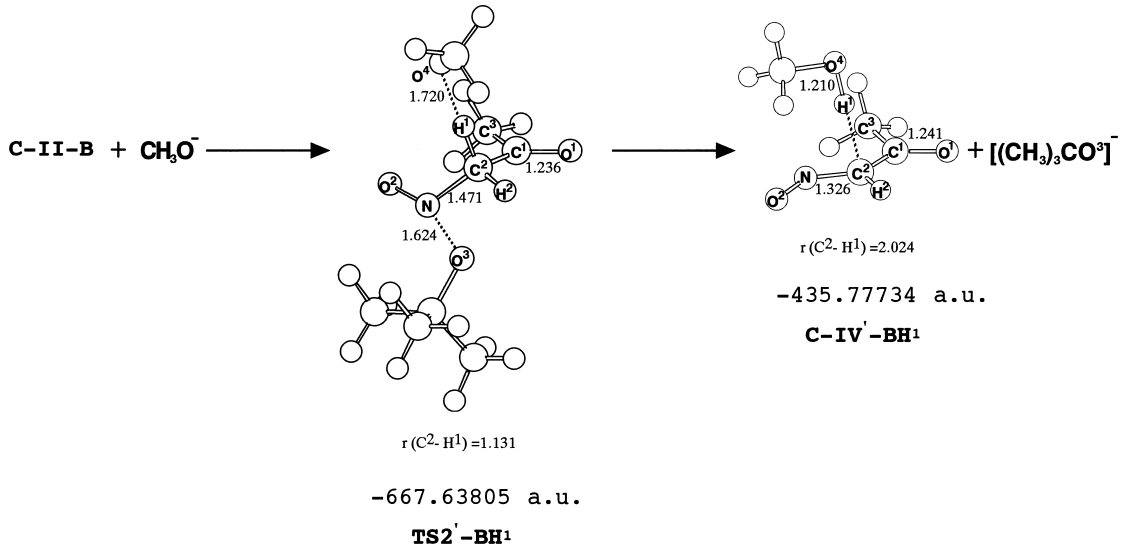

Fig. 8. Elimination Process of H^1 in C-II-B with CH_3O^-

counter-cation, theoretical expectations were experimentally substantiated by the formation of the *E*-oxime *via* nitrosation of acetone in a protic solvent.[7)]

The optimized conformations of each complex in this paper are similar to those of **1** with methyl nitrite.[1,2)] The bulkiness of the $(CH_3)_3C$ group did not greatly influence the *E*/*Z* ratio in the nitrosation of **1**. The steric effect of the $(CH_3)_3C$ group of **3** on the *E*/*Z* ratio was observed for reactions with ketones having bulky substituents such as isovalerophenone **5** ($C_6H_5COCH_2CH(CH_3)_2$). Accordingly, MO calculations of the nitrosation of **5** with **3** will be reported at a later date.

Acknowledgments The authors thank the Information Technology Center of Fukuoka University for the use of the Fujitsu GP7000S1000 computer, the Computing and Communications Center, Kyushu University for use of the Fujitsu VPP5000/64 computer, and to the Research Center for Computational Science, Okazaki National Research Institutes for the use of the NEC SX5 and Fujitsu VPP5000 computers.

References and Notes

1) Niiya T., Ikeda H., Yukawa M., Goto Y., *Chem. Pharm. Bull.*, **45**, 1387—1392 (1997).
2) Niiya T., Ikeda H., Yukawa M., Goto Y., *Chem. Pharm. Bull.*, **49**, 473—475 (2001).
3) Niiya T., Ikeda H., Yukawa M., Goto Y., *Chem. Pharm. Bull.*, **50**, 1502—1506 (2002).
4) Frisch M. J., Trucks G. W., Schlegel H. B., Scuseria G. E., Robb M. A., Cheeseman J. R., Zakrzewski V. G., Montgomery J. A., Jr., Stratmann R. E., Burant J. C., Dapprich S., Millam J. M., Daniels A. D., Kudin K. N., Strain M. C., Farkas O., Tomasi J., Barone V., Cossi M., Cammi R., Mennucci B., Pomelli C., Adamo C., Clifford S., Ochterski J., Petersson G. A., Ayala P. Y., Cui Q., Morokuma K., Malick D. K., Rabuck A. D., Raghavachari K., Foresman J. B., Cioslowski J., Ortiz J. V., Baboul A. G., Stefanov B. B., Liu G., Liashenko A., Piskorz P., Komaromi I., Gomperts R., Martin R. L., Fox D. J., Keith T., Al-Laham M. A., Peng C. Y., Nanayakkara A., Challacombe M., Gill P. M. W., Johnson B., Chen W., Wong M. W., Andres J. L., Gonzalez C., Head-Gordon M., Replogle E. S., Pople J. A., "Gaussian 98," Revision A.9, Gaussian, Inc., Pittsburgh, PA, 1998.
5) Foresman, J. B., Frisch A. E., "Exploring Chemistry with Electronic Structure Methods," 2nd ed., Gaussian, Inc., Pittsburgh, PA, 1996.
6) Gronert S., *J. Am. Chem. Soc.*, **114**, 2346—2354 (1992).
7) Ikeda H., unpublished results: formation of 1-hydroxy-imino-2-oxopropane (**4**). Acetone (0.125 mol), *tert*-butylnitrite (**3**) (0.188 mol), CH_3ONa (0.500 mol) in CH_3OH; reaction temperature, 273 K. Yield: **4***E* (14.2%), **4***Z* (0%).